

# CODAR Wave Measurements From a North Sea Semisubmersible

BELINDA J. LIPA, DONALD E. BARRICK, SENIOR MEMBER, IEEE, JAMES ISAACSON, AND  
PETER M. LILLEBOE

**Abstract**—CODAR, a high-frequency (HF) compact radar system, was operated continuously over several weeks aboard the semisubmersible oil platform *Treasure Saga* for the purposes of waveheight directional measurement and comparison. During North Sea winter storm conditions, the system operated at two different frequencies, depending upon the sea state. Wave data are extracted from the second-order backscatter Doppler spectrum produced by nonlinearities in the hydrodynamic wave/wave and electromagnetic wave/scatter interactions. Because the floating oil rig itself moves in response to long waves, a technique is developed and successfully demonstrated that eliminates to second order the resulting phase-modulation contamination of the echo, using separate accelerometer measurement of the platform's lateral motions. CODAR waveheight, mean direction, and period are compared with data from a Norwegian directional wave buoy; in storm seas with waveheights that exceeded 9 m, the two height measurements agreed to within 20 cm rms, and the mean direction to better than 15° rms.

## I. INTRODUCTION

WAVE MEASUREMENTS from offshore platforms are important for design purposes as well as for operational safety and efficiency. Measurement devices in the water are costly to deploy and maintain, thereby emphasizing the desirability of platform-mounted remote-sensing systems. One such device is CODAR, a high-frequency radar system which operates continuously and automatically. This paper describes an operational deployment of CODAR during November and December 1986 aboard the *Treasure Saga*, a semisubmersible oil exploration platform which was drilling off the Norwegian coast.

The interpretation of the data from a floating rig such as this requires consideration of the effects of platform motion that modify the received radar signal's frequency spectrum. In the absence of motion this radar spectrum consists of dominant peaks due to first-order Bragg scatter (i.e., echo diffracted from those waveheight spectral components half the radar wavelength moving towards and away from the radar), surrounded by a higher-order continuum which contains the wave information. Platform motion causes sidebands of the first-order echo to be superimposed on the continuum; methods are developed and demonstrated here that remove these contaminating rig-motion contributions. The platform displacement spectra measured by accelerometers mounted on the rig are input into an algorithm which removes their convolutional contamination. The resulting deconvolved spectrum

is then inverted to give parameters of the ocean wavefield, which are compared with simultaneous measurements made by a pitch/roll wave buoy operated by the Continental Shelf and Petroleum Technology Research Institute (IKU).

In this paper, we describe in Section II the deployment of the CODAR system and the accelerometers on the platform; the methods used to obtain and interpret the spectra of the radar signal and the platform motion are described in Section III; and radar results are compared with buoy measurements in Section IV.

## II. DESCRIPTION OF MEASUREMENT SYSTEMS

CODAR was originally developed as a coastal real-time surface-current mapping system by the present authors at the National Oceanic and Atmospheric Administration (NOAA) nearly 15 years ago [1], [2], and it operated at 25.4 MHz for this purpose; later it was extended to measure the on-shore coastal waveheight directional spectrum at this same frequency [3]–[5]. Under a four-year program the Gulf Oil Company, SAGA Petroleum A.S. of Norway, and CODAR Ocean Sensors Ltd. adapted this original hardware system to measure currents and waves from offshore oil platforms, both fixed and semisubmersible (floating) [6], [7]. Extraction of currents were discussed elsewhere [7], [8]; the present paper focuses on the wave measurements of CODAR from offshore platforms. Except for the antenna, the CODAR analog and digital hardware employed during these measurements is very similar to that used 10 years ago and discussed in [2], [6]. During the wave-measurement period of November and December 1986, the *Treasure Saga* was located in the North Sea directly north of Kristiansund, Norway, in the Haltenbanken field, at latitude 64° 56' 03.5" N and longitude 07° 39' 53.4" E. The water depth at the rig was 300 m; the closest land was nearly 120 km away. Although the *Treasure Saga* floats, its mooring holds it so that its mean bearing was observed to hold within 0.5° of true south. All CODAR equipment (consisting of two 1-m-high racks) except for the antenna was located on the bridge of the vessel.

A functional description and picture of the CODAR crossed-loop/monopole antenna system is found in [2]. The particular version used on the *Treasure Saga* stood about 2-m-high from its radial counterpoise base to the top of the loops; the whip monopole extended another 5 m, for a total monopole height of about 7 m. This crossed-loop/monopole system has its conducting elements enclosed in PVC and fiber glass plastics, weighs about 20 kg, and is designed to withstand (and actually did) gale-force winds of 50 m/s. The an-

Manuscript received January 16, 1989; revised October 10, 1989.  
The authors are with CODAR Ocean Sensors Ltd., P.O. Box 391087,  
Mountain View, CA, 94039-1087.  
IEEE Log Number 8933340.

tenna system is mounted at the top of the derrick in the middle of the rig at a height above mean sea level of  $\sim 105$  m. After lightning damage during operation in the previous year, the electronics at the antenna were redesigned to withstand the typical marine electrical discharge environment. Omnidirectional transmission takes place from the monopole, which is tuned for efficient radiation at the two CODAR frequencies (25.4 and 6.8 MHz). Reception takes place on both loops and the monopole elements. Although the loops are resonated at both operating frequencies, their efficiency is lower at 6.8 MHz (about 25-dB less than a quarter-wave monopole); however, since external noise in this lower HF region exceeds internal noise by 40–50 dB, this inefficiency does not ultimately degrade the system's signal-to-noise ratio (SNR). During early operations from offshore rigs it was discovered that significant pattern distortion can result from the inevitable metallic structure in the near field of the antenna; hence, methods were developed to (i) better isolate the antenna from the rig metal, primarily by mounting the antenna as high as possible and using ferrite chokes on nearby conductors to minimize current pickup, and (ii) measure and remove any remaining pattern distortion [8]. These methods were applied successfully in the algorithms used here.

This older version of CODAR employs a standard uncompressed, pulsed-signal format. Although capable of 10-kW peak power emission, an adequate SNR for nearby wave measurements was obtained during this period with only 2-kW radiated peak power at 25.4 MHz and with 1 kW at 6.8 MHz. (Since wave data near the rig were desired, data from range cells out to  $\sim 15$  km were employed for these tests.) Using a pulse width of  $8 \mu\text{s}$ , we realize a range cell width of 1.2 km. The pulse transmission repetition interval is  $512 \mu\text{s}$ . The returning data stream-out to 76.8 km is then sampled 64 times at an  $8\text{-}\mu\text{s}$  rate within this  $512\text{-}\mu\text{s}$  interval on one of the three antennas; then the receive signal from the second antenna is sampled over the next  $512\text{-}\mu\text{s}$  interval. Allowing for a blank  $512\text{-}\mu\text{s}$  interval for internal noise measurement after all three antenna elements are sampled, the multiplex time to revisit each receive antenna element is  $2048 \mu\text{s}$ . This revisit time is sufficiently fast so that sea-surface motions are frozen during this interval and the sequential measurements are essentially simultaneous. After careful transmit bandpass filtering at the antenna, the radiated signal spectrum from CODAR was monitored to ensure that it did not interfere with other radio users on the same rig, on other rigs nearby, and onshore.

Originally designed to operate for current measurement at 25.4 MHz, it was discovered several years ago that attempts at extracting wave information from the higher-order sea echo during high sea states will fail because of the breakdown of perturbation theory on which the mathematical inversion techniques are based [9]. Therefore, the program to adapt CODAR to open-ocean monitoring from oil rigs converted the hardware (and software) to dual-frequency operation. When significant waveheights fall below 4 m, the normal 25.4-MHz frequency is used. Above this waveheight the system switches to 6.8 MHz. (Occasional lower waveheight measurements were taken purposely at 6.8 MHz to verify low-frequency extracted waves.) Except for the first 2–3 week setup and checkout

phase, CODAR operated automatically, taking data every 3 h over a 36-min period, as described below. Radar system control and data preprocessing were done with a DEC PDP 11/23 microcomputer.

The measurement of four components of acceleration is required to remove the horizontal displacements of the rig (in response to the longer waves impacting it) that distort the phase of the CODAR sea-backscatter signal. These are surge, sway, pitch, and roll. We employed compact ( $20 \times 10 \times 10$  cm size) Systron-Donner units for this purpose whose analog outputs were sampled at precisely the 0.262144-s rate of the CODAR sea-echo time-series output. We did extensive tests on these units to verify the manufacturer's calibrations and found them to be correct; these were subsequently used in the software algorithms described below. Theoretically, the accelerometers must sense the motion-induced phase distortion *at the antenna*. However, by employing accelerometers both at the antenna (at the top of the derrick) and on the bridge of the rig (some 60-m apart), we observed that their simultaneous outputs at the low-frequency rig responses—over a period of many weeks—were essentially identical. Hence we used only the accelerometer outputs from the bridge for the measurements reported herein.

### III. INTERPRETATION OF CODAR AND ACCELEROMETER DATA

In this section we describe the signal analysis methods: First, the spectral analysis of the time series measured by the different sensors; then the interpretation of the spectrum in the absence of platform motion; and finally the method used to eliminate the platform-motion contribution to the spectrum.

#### A. Spectral Analysis and Calibration

1) *CODAR Data*: The complex voltage time series from the three CODAR antennas were fast-Fourier transformed (FFT) after applying a four-term Blackman-Harris window [10]; this reduces sidelobes by 92 dB from the main lobe maximum. Fifteen 4.5-min time-series segments, overlapped by 50%, were included in each 36-min data run every 3 h. The FFT that was done on time-series samples every 0.26 s resulted from digitally averaging 128 pulses every  $2044 \mu\text{s}$ , essentially a low-pass filtering process. Because of 90% correlation between adjacent frequency pair points produced by the heavy Blackman-Harris window, every other frequency point was omitted; the resulting frequency resolution was 0.00745 Hz. Individual 1.2-km adjacent range cells were averaged, to give a final range resolutions of 2.4 km. Cross spectra for the three antenna elements are then formed, averaged over the 36-min run and adjacent range cells; the amplitude of the antenna patterns is adjusted to be equal at their beam maximum, and relative phase corrections are applied to equalize the phase paths, using the method described by Lipa and Barrick [2].

2) *Accelerometer Data*: Four real time series are output from the accelerometer system: Surge  $s_x(t)$ , sway  $s_y(t)$ , pitch  $\theta_x(t)$ , and roll  $\theta_y(t)$  versus time  $t$ ;  $s_x$  and  $s_y$  represent the platform's accelerations to the south and east, respectively, and  $\theta_x$ ,  $\theta_y$  are its angular rotations (pitch and roll) as measured by electronically double-integrated angle accelerometers. Adding the term due to the gravitational acceleration  $g$ ,

the total accelerations in the south/east directions for pitch/roll angles less than  $5^\circ$  (which was always the case) are given by

$$\begin{aligned} a_x &\approx s_x + g\theta_x \\ a_y &\approx s_y + g\theta_y. \end{aligned} \quad (1)$$

FFT's of these signals are then formed after applying a Blackman-Harris window; frequency-dependent calibration factors (supplied by the manufacturer and verified by our own laboratory tests) are applied; and cross spectra among  $a_x$  and  $a_y$  are formed. The time sampling, time-series lengths, overlapping, and time averaging are exactly the same as used for CODAR data and described in the preceding section. Double integration with respect to time was accomplished by the multiplication of each frequency point in the cross spectra by  $1/\omega^4$ , where  $\omega$  is the angular spectral frequency. Before this frequency division, the acceleration spectra were truncated at frequencies less than 0.05 Hz to avoid the amplification of low-frequency noise by the integration process. The final result is the formation of the cross spectra between the horizontal displacements  $p_{xx}(\omega)$ ,  $p_{xy}(\omega)$ , and  $p_{yy}(\omega)$ .

### B. Radar Spectral Coefficients with No Platform Motion

The interpretation of the radar spectrum is based on Barrick's equations [11], [12] defining the narrow-beam radar return in terms of the waveheight directional spectrum. The Doppler spectrum consists of two dominant first-order peaks at the Bragg frequencies  $\pm \omega_B$  surrounded by a continuum, with

$$\omega_B = \sqrt{2gk_0} \quad (2)$$

for deep water, where  $k_0$  is the radar wavenumber, and  $g$  is the gravitational acceleration.

The CODAR receiving antenna consists of two crossed loops and a monopole [2], [3]. Signals from these elements are combined in the software to effect the azimuthal rotation of a broad-beam pattern, shaped like  $\cos^4(\phi/2)$ . The broad-beam radar sea-echo spectrum at scan angle  $\psi$  and Doppler shift  $\omega$  from the carrier, expressed as the radar cross section per unit area surface area per rd/s bandwidth, is given by the convolution of the antenna pattern and the narrow-beam radar cross section at bearing  $\phi$  (quantities with and without a wavy overbar denote broad-beam and narrow-beam sea echo, respectively):

$$\bar{\sigma}(\omega, \psi) = \frac{1}{2\pi} \int_{-\pi}^{\pi} \cos^4\left(\frac{\psi - \phi}{2}\right) \sigma(\omega, \phi) d\phi. \quad (3)$$

As shown by Lipa and Barrick [2], [3], (3) can be expressed as an angular Fourier series with five nonzero coefficients:

$$\bar{\sigma}(\omega, \psi) = \sum_{n=-2}^2 b_n(\omega) t f_n(\psi) \quad (4)$$

where the trigonometric functions are defined by

$$t f_n(\alpha) = \begin{cases} \cos(n\alpha), & n \geq 0 \\ \sin(|n|\alpha), & n < 0 \end{cases}. \quad (5)$$

The coefficients  $b_n(\omega)$  can be obtained from the broad-beam return, as described in [2], and are related to the narrow-beam radar cross section  $\sigma(\omega, \phi)$  at angle  $\phi$  by the following equation:

$$b_n(\omega) = \frac{a_n}{2} \int_{-\pi}^{\pi} \sigma(\omega, \phi) t f_n(\phi) d\phi \quad (6)$$

where  $a_{-2} = a_2 = 1/8$ ;  $a_{-1} = a_1 = 1/2$ ; and  $a_0 = 3/8$ .

Barrick's equations in [11] and [12], repeated as [13, equations (1) and (3)], give  $\sigma(\omega, \phi)$  in terms of the waveheight directional spectrum which we express as a Fourier series over angle with coefficients that are functions of the ocean radian wave frequency  $\omega$ :

$$\sigma(\omega, \phi) = \sum_{n=-2}^2 c_n(\omega) t f_n(\phi). \quad (7)$$

Estimates of the first five Fourier coefficients are then obtained by inverting the integral equation (6) as described in [13].

### C. Inclusion of Platform Motion Effects

We consider here the operation of CODAR from a semisubmersible platform which moves in response to long-period waves that impact upon it. The platform motion is measured by the accelerometer and converted to spectra of the displacement, as described in Section III-A. We now derive an expression for the measured radar spectrum in terms of the ocean wave spectra and spectra of the platform displacement. We start the analysis in the time domain where we can write the following fundamental equation describing the broad-beam complex voltage  $\bar{v}(t, \psi)$  at time  $t$  in terms of the narrow-beam complex signal  $v(t, \phi)$  and platform horizontal displacement vector  $\mathbf{r}(t)$  as a function of time:

$$\bar{v}(t, \psi) = \frac{1}{2\pi} \int_{-\pi}^{\pi} \cos^2\left(\frac{\psi - \phi}{2}\right) e^{i2\mathbf{k}_0 \cdot \mathbf{r}(t)} v(t, \phi) d\phi \quad (8)$$

where  $\mathbf{k}_0$  is the radio wavevector. Note that the cosine factor is squared in (8), in contrast to (3), representing voltage rather than power. The exponential factor that accounts for the platform motion represents a phase modulation of the echo signal. (Amplitude modulation on the signal due to antenna rotation through the  $< 5^\circ$  pitch/roll angles is negligible; the loop patterns are unchanging, while the monopole varies with the cosine of pitch/roll.) The mean value of  $\mathbf{r}(t)$  is taken to be the coordinate origin; i.e., the position the platform would come to rest in the absence of motion due to waves.

We will now give a brief description of approximate methods to remove the effects of platform motion, using accelerometer measurements of the displacement spectra. Simplification is possible in the statistical averaging of the voltage sea echo: averaging of the exponential factor is performed independently from the averaging of the narrow-beam sea echo voltage. This is justified physically, since the sea echo is due to Bragg scatter from the first-order ocean waves (6-m-long at 25.4 MHz) that are in a range cell several kilometers from the platform. However, the randomness in the exponential factor comes from the platform displacement  $\mathbf{r}(t)$ , which is

due to the long high waves impacting at the platform. Hence these two processes are statistically independent. After conversion to the frequency domain, the Fourier angular coefficients are derived; here we find it more convenient to use the complex exponential form (denoted by the over-dot) instead of the trigonometric form used in (6); these are defined by

$$\dot{b}_n(\omega) = \frac{a_n}{2} \int_{-\pi}^{\pi} \sigma(\omega, \phi) e^{in\phi} d\phi. \quad (9)$$

These complex exponential coefficients are easily expressed in terms of the real trigonometric coefficients defined by (6) and vice versa; e.g.,

$$\dot{b}_2(\omega) = b_2(\omega) + b_{-2}(\omega). \quad (10)$$

The relation between the coefficients  $\dot{b}_n(\omega)$  measured in the presence of platform motion and the desired uncontaminated coefficients  $\dot{b}_n(\omega)$  is obtained by the following procedure: (i) Equation (8) is multiplied by its complex conjugate, and its ensemble average is taken to give the voltage correlation function; (ii) the random voltage signals  $v(t, \phi)$  and  $r(t)$  are assumed to be statistically independent because the former results from short Bragg waves at the scattering circle approximately 5–6 km from the platform, while the latter results from long waves impacting the platform; (iii) in averaging under the integral sign, the Gaussian nature of the sea waveheight to first order (and thence  $r(t)$  in the exponential phase modulation factor) is used to write its Gaussian characteristic function resulting from its appearance in the complex exponential; (iv) the Gaussian joint characteristic function is expanded in its series, with terms (involving the platform-motion phase modulation) retained to second order; (v) its Fourier transform from the time-lag domain to the frequency domain is taken with the broad-beam and narrow-beam voltage spectra being expressed as  $\bar{\sigma}(\omega, \psi)$  and  $\sigma(\omega, \phi)$ , respectively; and (vi) equations (4)–(9) are used to expand the spectra into their complex exponential angular Fourier coefficients. The result—to second order—is

$$\frac{b\dot{p}_n(\omega)}{a_n} = \dot{b}_n(\omega) - \frac{k_0^2}{4} \begin{pmatrix} \gamma_2 \dot{b}_{n-2}(\omega) + 2\gamma_0 \dot{b}_n(\omega) + \gamma_{-2} \dot{b}_{n+2}(\omega) + \\ -\Gamma_2(\omega) \otimes \dot{b}_{n-2}(\omega) - 2\Gamma_0(\omega) \otimes \dot{b}_n(\omega) - \Gamma_{-2}(\omega) \otimes \dot{b}_{n+2}(\omega) \end{pmatrix} \quad (11)$$

where  $\otimes$  denotes convolution. In this equation the functions  $\Gamma_{-2}(\omega)$ ,  $\Gamma_0(\omega)$ ,  $\Gamma_2(\omega)$  are defined in terms of the accelerometer cross spectra through the equations,

$$\begin{aligned} \dot{\Gamma}_2(\omega) &= p_{xx}(\omega) - p_{yy}(\omega) - 2ip_{xy}(\omega) \\ \dot{\Gamma}_0(\omega) &= p_{xx}(\omega) + p_{yy}(\omega) \\ \dot{\Gamma}_{-2}(\omega) &= p_{xx}(\omega) - p_{yy}(\omega) + 2ip_{xy}(\omega) \end{aligned} \quad (12)$$

and  $\gamma_{-2}$ ,  $\gamma_0$ , and  $\gamma_2$  are defined by

$$\begin{aligned} \dot{\gamma}_2 &= \delta_x^2 - \delta_y^2 - 2i\delta_x\delta_y\rho_{xy} \\ \dot{\gamma}_0 &= \delta_x^2 + \delta_y^2 \\ \dot{\gamma}_{-2} &= \delta_x^2 - \delta_y^2 + 2i\delta_x\delta_y\rho_{xy} \end{aligned} \quad (13)$$

where  $\delta_x$ ,  $\delta_y$  are the rms cartesian lateral displacements of

the floating platform, and  $\rho_{xy}$  is the correlation coefficient between them. These quantities are defined in terms of the accelerometer cross spectra as follows:

$$\begin{aligned} \delta_x^2 &= \int_{-\infty}^{\infty} p_{xx}(\omega) d\omega, & \delta_y^2 &= \int_{-\infty}^{\infty} p_{yy}(\omega) d\omega, \\ \delta_x\delta_y\rho_{xy} &= \int_{-\infty}^{\infty} p_{xy}(\omega) d\omega. \end{aligned} \quad (14)$$

Thus the total mean-square lateral platform displacement is given by

$$\delta^2 = \delta_x^2 + \delta_y^2. \quad (15)$$

Thus the effects of platform motion appear as a convolution which deposits spectral energy in the form of motion-induced sidebands of the dominant first-order echo. These sidebands are superimposed on the desired second-order sea-echo Doppler spectrum; their amplitude is calculated using accelerometer measurements and are subtracted. The resulting spectrum can then be treated as if no platform motion were present.

#### D. Example of Impact of Platform Motion

A floating platform responds to waves with spatial wavelengths longer than its lateral dimensions; i.e., with temporal periods for the *Treasure Saga* exceeding about 7 s. If the rig were totally unconstrained by the mooring and drifted like a surface particle on a long wave, its lateral displacement in deep water would be the same as the waveheight, since a surface particle in deep water executes a circular orbital motion as a wavetrain passes by. The mooring and rig inertia constrain it so that its rms lateral displacement  $\delta$  never exceeds the rms waveheight  $h$ ; the relationship between the two versus frequency defines the rig's transfer function (including mooring). For the longest waves  $\delta$  becomes nearly as large as  $h$ . In this case, one might expect the added contribution from the platform-motion phase modulation to be

nearly as large as the uncontaminated second-order sidebands themselves. Wave energy estimates extracted by inverting the second-order echo—without compensation—would then be too high by nearly a factor of two for the longer waves; the waveheight itself, which varies with the square root of wave energy, would be overestimated by  $\sim 40\%$ .

This is shown in Fig. 1 in which the upper curve is the significant waveheight at 25.4 MHz extracted from CODAR data *without the deconvolution compensation* discussed in the preceding paragraph. The lower curve is the “significant lateral displacement” of the platform, measured directly from the accelerometer outputs; this is related to the rms in the same manner as is significant to the rms waveheight (i.e.,  $D_s = 4\delta$ ;  $H_s = 4h$ ). The points are measurements of the significant waveheight from an uncalibrated laser/accelerometer non-directional sea-state measuring system installed on the *Treasure*

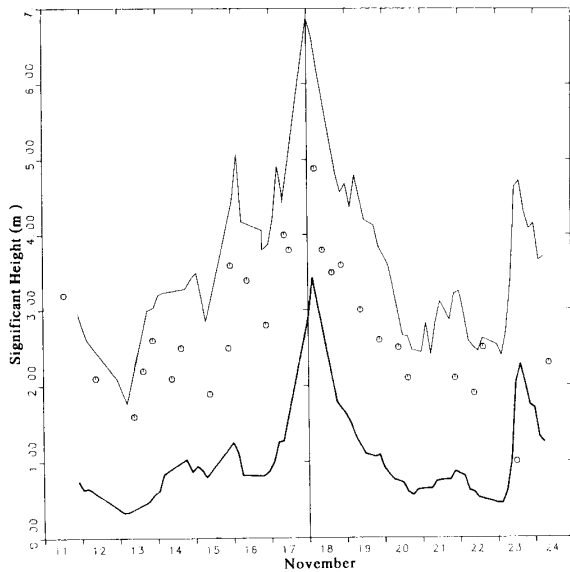


Fig. 1. Effect of platform motion on *Treasure Saga* on data. Upper curve is CODAR-extracted significant waveheight ignoring platform motion. Lower curve is the significant lateral displacement of the rig as measured by accelerometers. Points are estimates of significant waveheight from an uncalibrated laser wave-measuring system on the rig.

*Saga*. The curves clearly show that for the highest and longest waves, represented by the storm peak on November 17–18, 1986, uncompensated CODAR measurements are clearly too high by approximately 30%. On the other hand, the significant lateral displacement  $D_s$  is less than the other waveheight. There is clearly a correlation between the two over most of the record, the correlation being strongest for the longer period waves. The figure clearly demonstrates the point that platform motion cannot be ignored in the extraction of wave information from CODAR (or any Doppler radar measurements) or else significant errors will result. Accelerometers are perhaps the simplest method for removing motion effects entirely within the software.

#### IV. COMPARISON WITH SURFACE DATA

For verification of the radar results we used measurements made by an ODAS 492 directional wavebuoy operated at Haltenbanken by IKU; this buoy was approximately 15 km from the *Treasure Saga* at the time. These measurements include the significant waveheight, the dominant wave direction, and the mean spectral period. When available, we used data recorded on the buoy and processed onshore; IKU engineers confirmed [15] that preprocessed data on the buoy relayed by the ARGOS satellite were in error, underpredicting the waveheight and distorting the wave direction. However, for the second half of November the tape recorder aboard the buoy failed, and only preprocessed data transmitted via the ARGOS satellite was available. Also, only the peak period data are transmitted, which are statistically unstable and not suitable for comparison with the CODAR results. During this period we show the ARGOS significant waveheight and mean direction, but advise caution on its use for ground truthing.

The comparisons between the significant height, the mean spectral period, and the dominant wave direction are shown in Figs. 2–4. In these figures CODAR data are shown by circles (25.4 MHz) and crosses (6.8 MHz); buoy data are shown by the continuous lines—bold for data processed on shore, and fine for ARGOS-transmitted data. The CODAR-predicted waveheight agrees with the onshore-processed buoy waveheight to within 20 cm. CODAR waveheight is significantly greater than ARGOS-transmitted buoy data over periods from November 26 to December 1, 1986, during which the ARGOS significant waveheight is known to be too low. In the period for which comparable data are available, CODAR and buoy estimates of the mean wave period have an rms difference of 2 s; much of this variance appears to be due to the coarseness of the quantizing intervals used. During the observation period the dominant wave direction ranged over  $360^\circ$ ; the rms difference between the CODAR and buoy-measured direction is  $15^\circ$ .

#### V. DISCUSSION AND CONCLUSIONS

The results of extracting waveheight directional spectral parameters from CODAR data taken onboard a semisubmersible platform are very promising. Comparisons with a nearby directional wavebuoy over a one-month period are the basis of the evaluation made here, although the buoy cannot be considered “truth” because of its own biases [14]. Favorable agreement demonstrates that residual antenna-pattern distortion caused by near-field metallic obstacles can indeed be compensated for in software. The data here comprise the first CODAR wave measurements in which two widely spaced frequencies (25.4 and 6.8 MHz) were successfully employed, both producing wave parameters with reasonable accuracy. High wave conditions that were encountered during two North Sea storms necessitated the use of the lower frequency, as the sea echo saturates (or becomes insensitive) to higher waveheights.

The present data analysis also demonstrates that platform-motion contamination encountered by a wave radar on any floating semisubmersible or drill ship produces severe biases if ignored. This contamination is simply and successfully removed by using accelerometers. A physical algorithm involving a straightforward convolution/matrix-subtraction in the frequency domain is applied. An earlier approach based upon a full deconvolution in the time domain was attempted by using the accelerometer signals; this proved to be unsuccessful because matrix sizes that had to be inverted were very large, and the randomness of the signal caused insurmountable instabilities.

Fairly extensive operational experience with CODAR on an offshore oil platform (as well as coastal experience) suggests two improvements that will be incorporated in future designs: (a) Dual-frequency operation (to avoid saturation during high sea states), although it works, is a cumbersome, costly, and unnecessary feature. A compromise operation at a single frequency near 12 MHz—along with a minimal asymptotic extension of the inversion theory to handle extremely high sea states—seems to be a much sounder solution to the problem. Somewhat greater maximum distance is achieved due

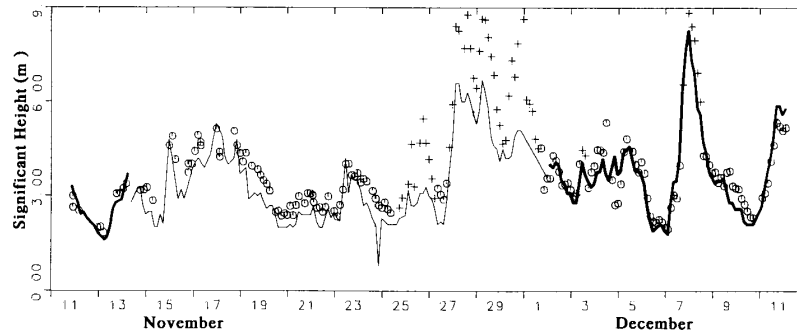


Fig. 2. Comparison of significant waveheight measured by CODAR and the IKU wavebuoy from November 11 to December 11, 1986. The continuous line represents the buoy measurement: bold—onshore processing; fine—ARGOS processed. Individual points represent CODAR results: o—25.4 MHz; +—6.8 MHz radar frequency.

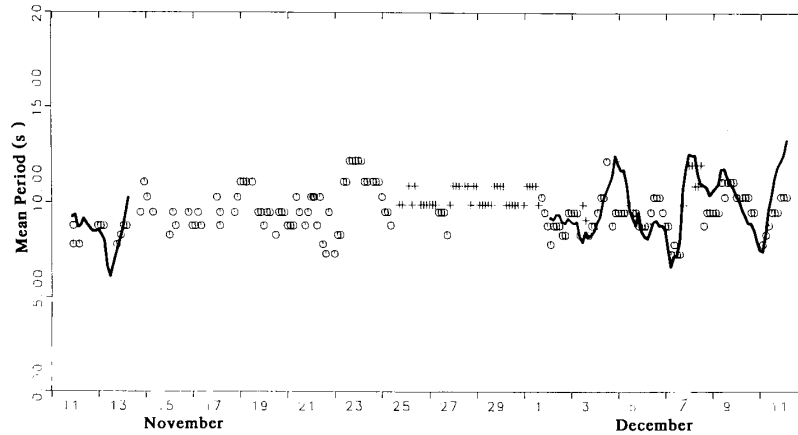


Fig. 3. Mean period comparison. The definition of lines and points are as in Fig. 2.

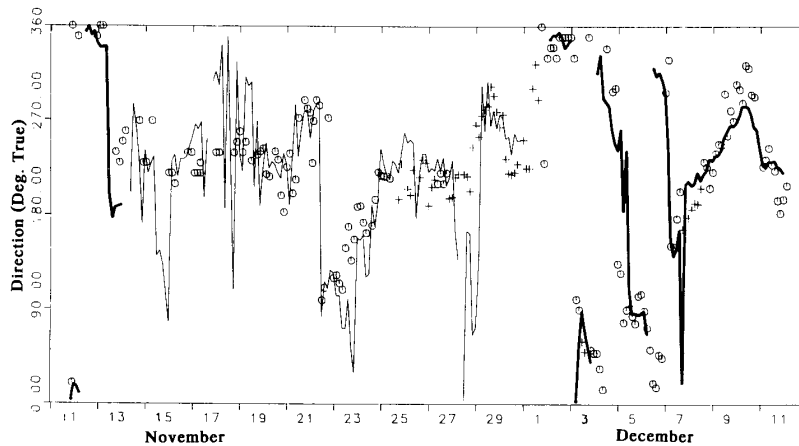


Fig. 4. Mean wave direction comparison. The definition of lines and points are as in Fig. 2.

to less path loss at the lower frequency. No sacrifice in accuracy is expected for surface-current mapping; and (b) the high peak radiated power used in our pulse-signal format can be avoided with no degradation in the signal-to-noise ratio (and hence maximum range) by switching to a more efficient, higher duty-factor signal format. High peak power causes concern because of the possibility of corona arcing produced by the high voltages at antenna elements and the resulting

fire/explosion potential in an offshore oil exploration environment. A new solid-state system is under development and evaluation which uses a 40% duty-factor gated FMCW signal. In the latter the frequency is swept repetitively over a bandwidth corresponding to the desired range resolution, and the transmitter and receiver are gated on/off sequentially. Maximum power required to attain the same range drops from 10 000 W with the older system to about 70 W with the new.

## ACKNOWLEDGMENT

The authors are indebted for the support, patience, and encouragement from Saga Petroleum A.S. of Norway, in particular to A. J. Kjelaas, B. Braennstrom, and K. L. Erikson. They are grateful for assistance from T. Johanson and J. Aksnes of Crea Unique A.S. Continued unflinching interest and support from M. W. Spillane, formerly of Gulf Oil Company, are sincerely appreciated.

## REFERENCES

- [1] D. E. Barrick, M. W. Evans, and B. L. Weber, "Ocean surface currents mapped by radar," *Science*, vol. 198, pp. 138-144, 1977.
- [2] B. J. Lipa and D. E. Barrick, "Least-squares methods for the extraction of surface currents from CODAR crossed-loop data: Application at ARSLOE," *IEEE J. Oceanic Eng.*, vol. OE-8, pp. 226-253, 1983.
- [3] D. E. Barrick and B. J. Lipa, "A compact, transportable HF radar system for directional coastal wavefield measurements," in *Ocean Wave Climate*, M. D. Earle and A. Malahoff, Eds. New York: Plenum, 1979.
- [4] B. J. Lipa and D. E. Barrick, "CODAR measurements of the wave-height directional spectrum in shallow water," in *IEEE 1981 Int. Geosci. and Remote Sensing Symp. Dig.* (Washington, DC), 1981, pp. 1107-1113.
- [5] B. J. Lipa and D. E. Barrick, "CODAR measurements of ocean surface parameters at ARSLOE—preliminary results," in *IEEE Oceans '82 Conf. Rec.* (Washington, DC), 1982, pp. 901-906.
- [6] M. W. Spillane, O. H. Oakley, Jr., M. W. Evans, B. J. Lipa, and D. E. Barrick, "A program to develop Coastal Ocean Dynamics Applications Radar for offshore wave, current, and wind monitoring," in *Proc. Offshore Techn. Conf.* (Houston, TX), 1983, OTC 4590, pp. 87-94.
- [7] M. W. Spillane *et al.*, "Results of the CODAR offshore remote-sensing project," in *Proc. Offshore Techn. Conf.* (Houston, TX), 1986, OTC 5214, pp. 503-510 (Available from Marine Technology Society).
- [8] D. E. Barrick and B. J. Lipa, "Correcting for distorted antenna patterns in CODAR ocean surface measurements," *IEEE J. Oceanic Eng.*, vol. OE-11, pp. 304-309, 1986.
- [9] D. E. Barrick, "The role of the gravity-wave dispersion relation in HF radar measurements of the sea surface," *IEEE J. Oceanic Eng.*, vol. OE-11, pp. 286-292, 1986.
- [10] F. J. Harris, "On the use of windows for harmonic analysis with the Discrete Fourier transform," *Proc. IEEE*, vol. 66, pp. 51-83, 1978.
- [11] D. E. Barrick, "First-order theory and analysis of MF/HF/VHF scatter from the sea," *IEEE Trans. Antennas Propagat.*, vol. AP-20, pp. 2-10, 1972.
- [12] D. E. Barrick, "Remote sensing of sea state by radar," in *Remote Sensing of the Troposphere*, V. E. Derr, Ed. Washington, DC: GPO, 1972, ch. 12.
- [13] B. J. Lipa and D. E. Barrick, "Extraction of sea state from HF radar sea echo: Mathematical theory and modeling," *Radio Sci.*, vol. 21, pp. 81-100, 1986.
- [14] D. E. Barrick, B. J. Lipa, and K. E. Steele, "Comments on 'Theory and application of calibration techniques for an NDBC directional wave measurements buoy': Nonlinear effects," *IEEE J. Oceanic Eng.*, vol. 14, pp. 268-272, 1989.
- [15] A. J. Kjelaas, private communication.



**Belinda J. Lipa** was born in Bombay, India. She received the B.Sc. and Ph.D. degrees from the University of Western Australia in mathematics and theoretical physics in 1965 and 1969, respectively.

During 1972-1979 she worked as a Research Associate at Stanford University, developing methods for inverting integral equations to yield geophysical parameters and their uncertainties. She continued this work as a Senior Research Physicist at SRI International, Menlo Park, CA, until 1981, when she formed CODAR Research, where she developed analysis techniques and software for HF radars that measure ocean surface currents and waves; she continues this work at CODAR Ocean Sensors Ltd., Mountain View, CA, where she is currently Vice President for Systems Analysis and Modeling. She joined the Acurex Corporation part-time in 1987 as a Staff Physicist in the Electromagnetics Department. She presently works part-time in Mirage System's Research and Development Department

as Senior Scientist, developing software and modeling signal processing and data analysis for radar applications.

Dr. Barrick is a member of URSI Commission F and the American Geophysical Union.



**Donald E. Barrick** (M'62-SM'86) was born in Tiffin, OH. He received the B.E.E., M.Sc., and Ph.D. degrees in electrical engineering from The Ohio State University, Columbus, in 1961, 1961, and 1965, respectively.

He joined the staff of Battelle Memorial Institute in Columbus, OH, in 1965, where he led work in radar scattering and signal processing as an Institute Fellow until 1972. During this same period he taught electromagnetics and communications theory at The Ohio State University's Electrical Engineering Department as an Adjunct Assistant Professor. During 1972-1982 he served as Chief of the Sea State Studies Branch of the U.S. National Oceanic and Atmospheric Administration's Wave Propagation Laboratory in Boulder, CO; there he developed compact HF radar systems for real-time mapping of ocean currents and waves. Since 1982 he has worked in industry, heading CODAR Ocean Sensors Ltd., Mountain View, CA. In 1987 he joined Acurex Corporation part-time as Manager of the Electromagnetics Department. Since 1989 he has served as Mirage System's Chief Scientist. His interests include radar scattering and the development of compact radar systems with novel waveforms.

Dr. Barrick is a member of Sigma Xi, URSI Commissions F and C, the American Geophysical Union, and the American Meteorological Society; he has served as Associate Editor and Administrative Committee member for the IEEE Antennas and Propagation Society.



**James Isaacson** was born in Austin, TX. He received the B.A. degree in mathematics and the M.A. degree in numerical analysis from the University of Texas at Austin in 1963 and 1965, respectively, and the M.Sc. degree in computer science from North Texas State University, Denton, in 1977.

During 1965-1966 he worked as Programmer/Analyst at the Boeing Company in Huntsville, AL. During 1966-1968 he was Lead Programmer at Bell Helicopter in Euless, TX, and during 1968-1970 as Staff Analyst at the Computer Usage Company in Dallas, TX. During 1970-1976 he worked as Associate Professional Scientist at the Sun Oil Company in Richardson, TX. During the period 1976-1979 he taught Computer Science at North Texas State University and the University of Colorado, Boulder. During 1979-1982 he was Manager of Applications Programming at the Denver Processing Center, Denver, CO, and from 1982-1986 he was Director of Software at Codar Technology, Inc., Longmont, CO. Since 1986 he has served as Vice President for Software at CODAR Ocean Sensors Ltd., Mountain View, CA, and as a part-time Staff Engineer at the Acurex Corporation. His principal interests are real-time data acquisition software and instrument control, digital signal processing, software interfaces, and numerical analysis.

Mr. Isaacson is a member of DECUS (Digital Equipment Computer Users Society), SEG (Society of Exploration Geophysics), and ACM (Association for Computing Machinery).



**Peter M. Lilleboe** was born in Cannon Falls, MN. He attended the University of Colorado, Boulder, in electrical engineering and received the Associate degree in electronics from the Community College in Denver in 1982.

He served as RF Engineer at Codar Technology, Inc., Longmont, CO, during 1981-1986, where he installed and maintained HF radar systems for coastal and offshore oil platform applications; he engineered a unique compact three-element HF radar antenna. From 1986 to present he serves as Vice President of RF Systems at CODAR Ocean Sensors Ltd., Mountain View, CA. In this role he has designed and is co-inventor of a unique, ultra-compact, low-power HF radar system that employs high-duty-factor swept-frequency signal formats for ocean surface and surveillance applications. He joined the Acurex Corporation in 1987 as a Staff Engineer, where he designed and installed an indoor anechoic radar range. In addition to working at CODAR, he presently works part-time as an Engineer at Mirage Systems, where he designs and prototypes radars and other RF components that employ digital waveform control and signal processing.